Self-Healing Asphalt with Optimised Tyre-Based Pyro-Rejuvenator: A Multi-Scale Evaluation

Manuel Chávez-Delgado[a,b*], Jose L. Concha[a], Silvia Caro[c], Carlos P. Silva[d,e], Luis E. Arteaga-Pérez[f], Jose Norambuena-Contreras[g*]

[a] LabMAT, Departamento de Ingeniería Civil y Ambiental, Facultad de Ingeniería, Universidad del Bío-Bío, Concepción, 4051381, Chile

[b] Departamento de Ingeniería Civil, Facultad de Ingeniería, Sede Concepción, Universidad Andres Bello, Chile.

[c] Department of Civil and Environmental Engineering, Universidad de los Andes, Bogotá, Colombia

[d] Universidad de Santiago de Chile (USACH), Facultad de Química y Biología, Departamento de Química de los Materiales

[e] Soft Matter Research and Technology Center, SMAT-C, Santiago, Chile

[f] Department of Chemical Engineering, Faculty of Engineering, Universidad de Concepcion, Concepción, 4030000, Chile

[g] Advanced Bituminous Materials Laboratory, Department of Civil Engineering, Faculty of Science and Engineering, Swansea University, SA1 8EN, United Kingdom

*Corresponding authors: Manuel Chávez-Delgado; Jose Norambuena-Contreras

ABSTRACT

This study investigates an optimised pyro-rejuvenator (PR), derived from the pyrolysis of waste tyres, as a novel agent for self-healing asphalt. A multi-scale approach, encompassing chemical, microstructural, and mechanical evaluations, was employed to assess the effectiveness of the pyro-rejuvenator. The PR was incorporated into long-term aged bitumen (PAV) at dosages of 3 wt.% and 6 wt.%, with chemical changes analysed using Fourier transform infrared spectroscopy (FTIR), atomic force microscopy (AFM), and chemical fractionation (SARA). The self-healing performance of the treated and unaged bitumen was evaluated through fatigue-healing-fatigue tests using a dynamic shear rheometer (DSR) and tensile tests under static conditions. Additionally, the PR's efficacy was compared with a commercial rejuvenator. Results showed that PR's high content of alkenes and aromatics (e.g., limonene: 32.9%, cymene: 20.65%) facilitated the restoration of the maltenic fraction in bitumen and enhanced chemical interactions with the treated material. These compounds also promoted the pepticising

effect on the "bee-like" structures, leading to a more homogeneous microstructure. Under optimal conditions (6 wt.% PR dosage and 30 °C), a fatigue healing index of 30% was achieved, comparable to virgin bitumen (31%). In tensile tests at 25 °C after 12 hours, the healing index matched that of the commercial rejuvenator. These findings highlight the potential of pyro-rejuvenators as a sustainable and effective solution for the functional restoration of aged bitumen.

Keywords: Self-Healing; Asphalt Rejuvenator; Tyre Pyrolytic Oil; Cracking; Atomic Force Microscopy.

1. INTRODUCTION

Asphalt mixtures play a key role in pavement construction as they are essential to ensure the durability and strength of road surfaces. However, throughout their service life asphalt pavements are exposed to varying traffic loads, thermal stresses and environmental factors that trigger bitumen ageing processes [1,2]. Bitumen is a viscoelastic complex fluid which plays a binder role in asphalt mixture composition, and it is composed of four major organic SARA fractions grouped as Saturates, Aromatics, Resins and Asphaltenes. Due to its organic nature, the less stable fractions of bitumen (i.e., Saturates and Aromatics) are prone to volatilisation and oxidation during the operation of asphalt roads [3,4].

This chemical alteration modifies the balance of SARA fractions, along with an increase in the carbonyl and sulfoxide functional groups in the bitumen, which subsequently causes the agglomeration of asphaltene molecules [5,6]. As a result, the stiffer aged bitumen experiments an increase in the rutting resistance, but a loss of its original physical, rheological, and mechanical properties, along with its intrinsic self-healing capability [7,8]. These changes have a negative effect on asphalt roads, such as reduced resistance to fraying, fatigue and thermal cracking [1]. This degradation not only compromises driving comfort and reduces the pavement's service life but also increases the economic costs of road maintenance [9].

The application of rejuvenation agents offers a promising solution to counteract the adverse effects of asphalt pavement ageing [10,11]. These agents chemically interact with bitumen, altering and enhancing its physical, mechanical and rheological properties [12,13]. The purpose of the rejuvenator is to diffuse into the asphalt matrix, softening it and compensating for the losses suffered during the ageing process [14]. This enables the bitumen to

regain its ability to flow through micro-cracks, facilitating their self-healing and extending the service life of asphalt pavements [9,15]. Furthermore, the use of rejuvenators enables the incorporation of high percentages of Reclaimed Asphalt Pavement (RAP > 30% by weight of the total asphalt mixture), which significantly reduces maintenance costs and decreases the consumption of non-renewable resources [16]. Nonetheless, concerns over the environmental impact of rejuvenators, which are primarily derived from petroleum distillation, have driven the search for more sustainable and eco-friendly alternatives [14,17].

In this context, researchers worldwide have been exploring various bitumen-miscible agents as potential rejuvenators to restore the original properties of bitumen. These agents include sunflower several vegetable-based oils, as well as recycled vegetal and mineral oils [13,18]. Similarly, recent years have seen a growing scientific and technological interest in the thermochemical conversion of waste to produce new materials through processes such as pyrolysis, gasification, and liquefaction [19–23]. In this context, waste tyres are gaining recognition as a potential source for new waste-based rejuvenators derived from pyrolysis [14,24,25].

Pyrolysis is a thermochemical decomposition process that occurs in an oxygen-depleted environment at relatively high temperatures of 400 $<T_{pyro}<$ 700 ºC. The pyrolysis of waste tyres produces three fractions: liquid (known as Tyre Pyrolytic Oil), a solid enriched in carbon (known as recovered carbon black) and pyrolytic gas with a high heating value. The yield and composition of these fractions are influenced by the polymeric composition of the waste tyres as well as the operational conditions, particularly pyrolysis temperature, residence time, and condensation conditions.

Tyre pyrolytic oil (TPO) is a brown liquid with physical properties, such as density and viscosity, comparable to those of diesel fuel, and it contains various chemical families. For example, Martínez et al. [26], Campuzano et al. [27] , Chavez-Delgado et al. [14] and Menares et al. [24], demonstrated that pyro-oils contain a cocktail of terpenic compounds, such as limonene and cymenes, as well as alkylbenzenes, alkenes, alkanes, and heavier hydrocarbons, all of which hold potential applications. Particularly in rejuvenating aged bitumen, this complex chemical composition of TPO is of special interest. As shown in Figure 1, the compounds present in TPO could compensate for the chemical fractions lost during the bitumen oxidation process (mainly saturates and aromatics), thus helping to restore the balance between asphaltenes and maltenes. This recovery of the chemical balance could favour

molecular interactions that enhance the pepticising effect in the agglomeration mechanisms of the aged bitumen molecules, promoting the recovery of its physical, mechanical, rheological, and self-healing properties [28–30].

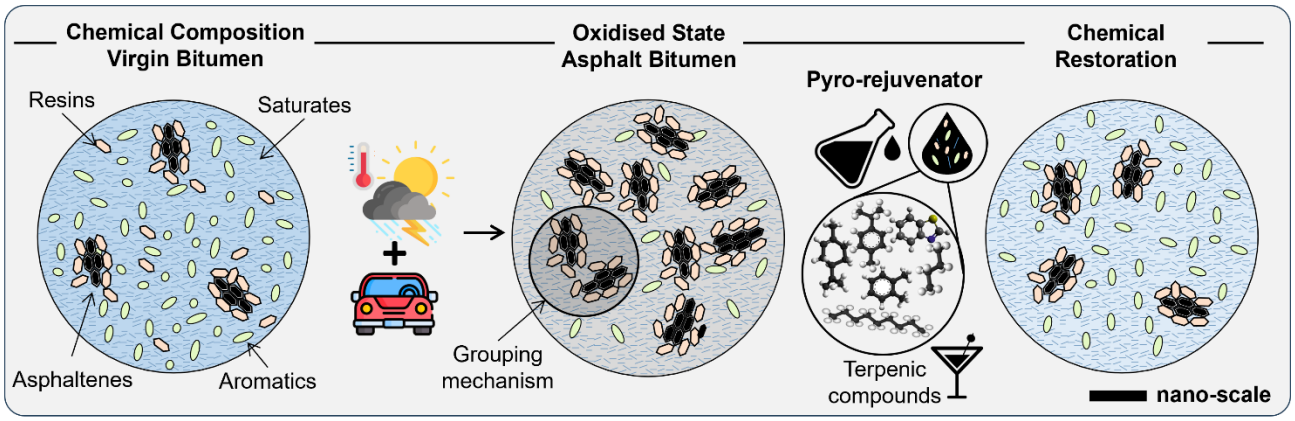

Figure 1. Molecular recovery mechanisms of aged bitumen by the effect of the pyro-rejuvenator.

Several investigations have explored the use of TPO as a potential rejuvenating agent for aged bitumen [14,31–40]. A study conducted by Fini et al. [36] revealed, based on Fourier Transformed Infrared spectroscopy (FTIR) and Thin-Layer Chromatography with Flame Ionisation Detection analysis, that TPO presented a high content of aromatic compounds and relatively low levels of saturates, resins and asphaltenes. Furthermore, they demonstrated the effectiveness of these liquids in restoring the physical and rheological properties of aged bitumen.

Similarly, Avsenik et al. [41] and Kumar et al. [37,42] showed that additions close to 10 wt.% of TPO decreased the softening point and increased the penetration of aged bitumen. Besides, when they evaluated this TPO-doped bitumen through DSR testing, they observed that the aged bitumen was softened, and its stiffness decreased. Similarly, Al-Sebaeei et al. [43] added TPO and crude palm oil in aged bitumen and showed that the combination of these products improved the rutting, ageing and fatigue resistance of the aged bitumen. Recently, Chavez-Delgado et al. [44] demonstrated that the incorporation of 6% TPO, relative to the weight of aged bitumen, effectively restores its linear viscoelastic properties ($|G^*|$ and δ) to a state comparable to that of virgin bitumen, thereby confirming the efficacy of TPO as a rejuvenating agent.

While numerous studies have been conducted to analyse the effects of TPO on the chemical, physical, rheological, and mechanical modifications of bitumen, its self-healing capacity remains an underexplored aspect in the literature [25,45]. In a pioneering study, Norambuena-Contreras et al. [25] developed sodium alginate biopolymer

capsules containing a non-distilled TPO and evaluated their effect on the self-healing capacity of aged bitumen. The main results showed that TPO is an effective rejuvenating agent capable of diffusing into bitumen, reducing its viscosity and promoting the self-healing of microcracks. Although this previous research offers valuable insights, the self-healing phenomenon was initially examined by applying the TPO directly to the micro-crack rather than incorporating it into the aged bitumen, which may have influenced the results obtained. In addition, Liu et al. [45] employed a combination of TPO and pyrophosphoric acid (PPA) to evaluate their effects on the self-healing capacity of bitumen through time sweep experiments, demonstrating that TPO/PPA combinations significantly enhance the recovery of self-healing properties. However, the isolated effect of TPO on bitumen's self-healing properties was not investigated in the study.

Despite significant research advancements on the effects of TPO for bitumen self-healing, its industrial-scale application could pose challenges related to health, safety, and environment (HSE) issues [46]. In this regard, the presence of potentially toxic compounds, such as light aromatics, volatile organic compounds (VOCs), and polycyclic aromatic hydrocarbons (PAHs), should be considered during the design and application of pyro-rejuvenators [47,48]. In response to these concerns, various physical and chemical processes (e.g., distillation, liquid-liquid extraction, etc.) have been studied to optimise the composition of TPO and minimise the impact of hazardous compounds during the application of pyro-rejuvenators.

In this context, Chavez-Delgado et al. [14] developed a bitumen rejuvenator from waste tyre blends through pyrolysis, followed by atmospheric distillation of the crude TPO. This innovation, termed "pyro-rejuvenator" was obtained from the 160–200°C distillation cut, following a comprehensive analysis of several distillation fractions. The researchers found that volatile compounds in TPO were primarily concentrated in the light fraction (20–160°C), while PAHs were predominantly present in the heaviest fraction (<280°C). The authors argued that the PR has a high potential for enhancing the self-healing capacity of aged bitumen owing to its remarkably high contents of limonene (33.71 wt.%) and monoaromatics (52.92 wt.%).

Although significant advancements have been made in the use of TPO as a bitumen rejuvenator, research on the chemical, microstructural, and mechanical effects of a pyro-rejuvenator derived from TPO distillation on the self-healing properties of aged bitumen remains limited. The primary objective of this study is to evaluate the impact

of an optimised pyro-rejuvenator on the self-healing characteristics of aged bitumen, establishing direct correlations between its chemical composition, microstructural properties, and self-healing capacity. To achieve this, key variables were analysed through a multi-scale approach, covering chemical composition (assessed via FTIR-ATR spectroscopy and SARA fractionation), surface micromorphology (evaluated using AFM analysis), and self-healing capacity (measured through DSR fatigue-healing-fatigue tests under various time and temperature conditions, complemented by tensile tests to examine the mechanical aspects of healing). The effectiveness of the pyro-rejuvenator was compared to that of a commercial rejuvenator in terms of self-healing performance.

2. MATERIALS AND METHODS

2.1. Materials

In this study, a pyrolytic oil obtained by pyrolysis (465°C) of waste tyre blends and further distillation (cut 160-200 °C) was used as a potential rejuvenating agent for aged bitumen: named pyro-rejuvenator [14]. The potential of the PR to restore the self-healing capacity of aged bitumen was compared to a commercial rejuvenator (CR) primarily used in the local space. The physical properties of PR and CR are shown in Table 1.

Table 1. Physical properties of the rejuvenating agents.

Type of rejuvenator	Density (g/cm^3)	Viscosity at 20°C (mPa*s)	pH at 25°C	Cont. Water (%)
Pyro-Rejuvenator	0.868 ± 0.05	1.77	8.87 - 9.08	0.055 ± 0.003
Commercial Rejuvenator	0.870 ± 0.05	90	9.21 - 9.35	0.290 ± 0.01

Virgin bitumen, designated as binder CA-24 (PG 64-22) and referred to as unaged bitumen, was used to prepare short and long-term aged bitumen samples according to standard laboratory tests. Short-term ageing of virgin bitumen was performed using the Rolling Thin Film Oven (RTFO) test at 163 °C for 75 minutes, as per ASTM D 2872-19 [49]. To simulate long-term ageing, the Pressurised Air Vessel (PAV) test was performed at 100 °C for 20 hours, as specified by ASTM D 6521-19 [50]. The conventional physical properties of all the bitumens used in this study were determined and are presented in Table 2.

Table 2. Physical properties of unaged bitumen, RTFO, PAV, and PAV rejuvenated with pyro-rejuvenator (PAV+PR) and commercial rejuvenator (PAV+CR).

Characteristic	Units	CA-24/ PG 64-22			PAV + PR		PAV + CR	
		Unaged	RTFO	PAV	3 wt.%	6 wt.%	3 wt.%	6 wt.%
Penetration 25°C, 100 g. 5s	0.1 mm	53	28	18	31	58	33	57
Softening point	°C	52.2	58.4	65.8	58.4	53.6	58	51
Absolute viscosity 60°C	Pa·s	265	973	6260	1660	507	1330	367
Ductility	cm	150	100	3.4	70	150	90	150

2.2. Blending of the PAV-aged bitumen with the pyro-rejuvenator

The PR and CR oils were blended with PAV-aged bitumen to assess their rejuvenating impact on the aged material. To do so, 80 g of the PAV-aged bitumen was poured into a 100 ml glass-wide-mouth bottle, heated at 140 ºC using a heating plate and mechanically stirring at 300 rpm for 15 min. The temperature was selected due to the high stiffness of the PAV-aged bitumen and the need to achieve a viscosity level that would allow efficient mixing with the PR. During this process, PR and CR were added at two contents: 3 wt.% and 6 wt.% with respect to the total mass of the aged bitumen (see Figure 2). These doses were decided according with previous studies on the recovery of physical and rheological properties of aged bitumen modified with a PR reported by Chavez-Delgado et al. [14,44]. The resulting samples were hermetically sealed and labelled X-Y, where X represents the type of rejuvenator (PR or CR) and Y represents the rejuvenator dosage (3 and 6), respectively.

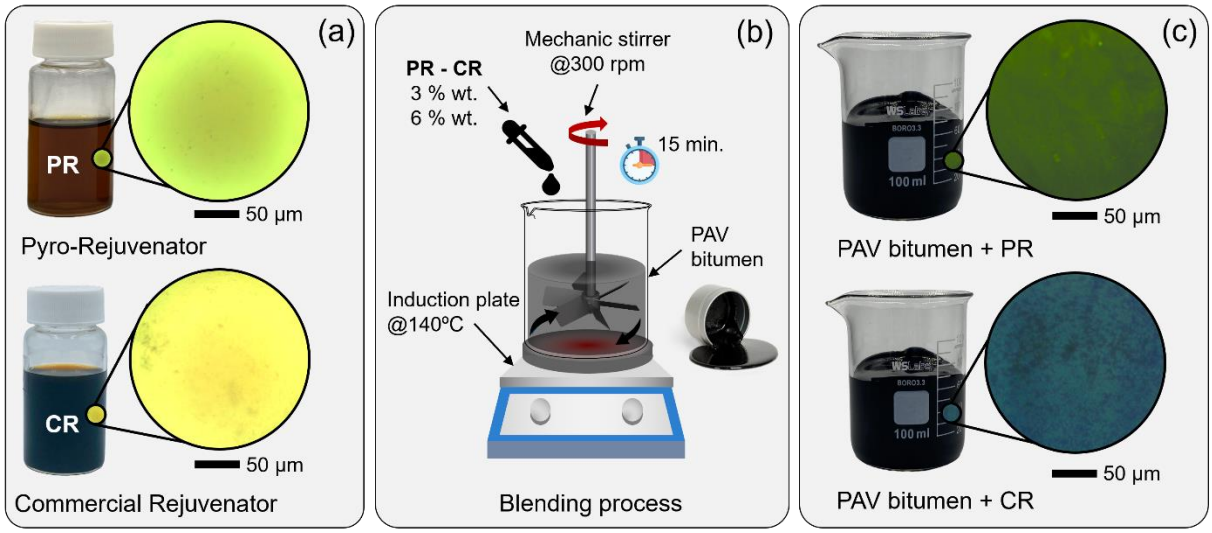

Figure 2. Blending of rejuvenating in PAV-aged bitumen. (a) rejuvenators used and their fluorescence microscope images; (b) the blending process on PAV-aged bitumen samples containing an optimum amount of rejuvenator; and (c) the corresponding blends of PAV-aged bitumen with rejuvenators and their fluorescence microscope images.

2.3. Chemical characterisation of the pyro-rejuvenator and bitumen

The bitumen samples utilised in this study were analysed to determine their chemical composition as Saturates, Aromatics, Resins, and Asphaltenes (SARA) using the modification of the ASTM D 4124-09 [51] method described by Concha et al. [52]. To separate the bulk maltenic fraction from the asphaltenes, n-heptane was used as the solvent in a standard reflux system. The maltenes were then separated into saturates, aromatics, and resins using column chromatography with solutions of n-heptane, methanol, and methanol/toluene at specific ratios. All reagents were obtained from Merck (Darmstadt, Germany) in analytical grade and utilised without additional purification. The unaged bitumen (CA-Virgin) and CA-PAV containing 0 wt.%, wt.% and 6 wt.% of PR per total mass of aged bitumen were analysed by FTIR-ATR to determine their specific ageing ratios by using spectroscopic descriptors.

The FTIR-ATR analysis was performed in a Nicolet is20 spectrometer interfaced with an Attenuated Total Reflection (ATR, Quest, Specac, UK) accessory with a Ge crystal. All the spectrums were averaged from 32 scans recorded in the mid-infrared region (400 – 4000 cm^{-1}) at a resolution of 4 cm^{-1}. The spectrums underwent baseline correction, area-based normalisation (reference peak at 2920 cm^{-1}), and multiple scattering correction to ensure unbiased comparison. Finally, the FTIR-ATR data was interpreted by well-known quantitative carbonyl and sulfoxide indices (Equations 1 and 2).

$$I_{C=O} = \frac{A_{1700}}{\sum_{i=0}^{n} A_n}: \text{ Carbonyl index} \quad (1)$$

$$I_{S=O} = \frac{A_{1030}}{\sum_{i=0}^{n} A_n}: \text{ Sulfoxide index} \quad (2)$$

where A represents the absorption area of a specific peak, and n corresponds to the areas of the peaks located at 720, 745, 815, 864, 1030, 1375, 1460, 1610, 1799, 2850, 2920 cm^{-1}.

The PR composition was analysed in a gas chromatograph (GC-2010 Plus, Shimadzu) interfaced with a single quadrupole mass spectrometry detector (QP 2010 Ultra, Shimadzu) (GC/MS). The specimens were separated using a 50-m-long ZB-5 capillary column with an internal diameter of 0.25 μm. In a typical analysis, 0.5 μL of sample were injected at a 1:100 split ratio into a split or splitless injection port that had been heated to 300 °C. The ion-

mass spectrums were matched to the National Institute of Standards and Technology database to identify the chemical species, considering a similarity index over 80%. The chromatograms underwent post-treatment to determine the product distribution based on area-selectivity, following the approach described by Menares et al. [24]. Considering the complexity of PR composition, it was also analysed by FTIR-ATR following the same procedures as described before for the bitumen.

2.4. Microstructural characterisation of bitumen using AFM

Atomic Force Microscopy (AFM) has emerged as a powerful tool for characterising the ageing process and modifications occurring in bitumens when treated with rejuvenators. Moreover, AFM has been used to explore the relationship between bitumen's self-healing properties and its morphological characteristics [47,53].

In this study, the surfaces of the bitumen samples were analysed by AFM in AC-mode using an AFM/SPM Controller 9500 Series system (Keysight Technologies, CA, USA) with a 7500 scanner. The surfaces were scanned at a scan rate of 0.3 Hz using a commercial Arrow NCR tip NanoWorld®, Switzerland (285 kHz nominal frequency, 42 N/m nominal spring constant). Images were processed and analysed using Keysight PicoView software. All bitumen specimens for AFM testing were prepared using the thermal approach, *i.e.* a drop of bitumen heated to 120°C was briefly poured onto an AFM steel disc inclined at 45 degrees and heated in an oven at a constant temperature of 120°C for approximately 5 minutes. Finally, they were cooled to room temperature and stored in a sealed container.

2.5. Self-healing level of the rejuvenated bitumen using a fatigue-healing-fatigue test via DSR testing

The self-healing level of the bitumen was measured through a fatigue-healing-fatigue test of bitumen in a DSR. After that, the self-healing performance of bitumens was evaluated by comparing the dynamic shear modulus change curve of the bitumens with the rejuvenators before and after a healing period.

The experimental parameters used in this study were as follows: The DSR was operated in time sweep mode, with a frequency of 10 Hz and a controlled shear strain of 10%. Three replicates were tested per material, and the average of the measurements was taken as the result, provided that the coefficient of variation was less than 10%. The test consisted of the following three steps (see Figure 3):

***Step 1. First fatigue*:** Each specimen was tested until producing a 50% drop in of the initial dynamic shear modulus $|G^*|_i$. The modulus after failure is referred to as $|G^*|_{(50\%)i}$.

***Step 2. Healing period*:** After the first fatigue stage (Step 1), the specimen was left in the rheometer for different healing times (10, 20 and 30 minutes) and temperatures (20, 25 and 30 °C). These parameters were defined as the resting period to allow the bitumen to heal.

***Step 3. Second fatigue*:** After the rest period (Step 2), the sample was subjected to a second fatigue test under the same conditions as in Step 1. The dynamic shear modulus measured after healing was designated $|G^*|_R$.

Finally, the healing index of the tested specimens under fatigue (HI_f) was calculated based on the methodologies proposed by Li et al. [54] and Wang et al.[55], using equation (3):

$$HI_f(\%) = \frac{|G^*|_R - |G^*|_{(50\%)i}}{|G^*|_i - |G^*|_{(50\%)i}} \quad (3)$$

where $|G^*|_i$ is the initial complex shear modulus at the start of the fatigue damage test, measured in kPa; $|G^*|_{(50\%)i}$ is the complex shear modulus at a specified level of reduction (50%), measured in kPa; and $|G^*|_R$ is the initial complex shear modulus at the start of the second fatigue damage test after a specified healing time and temperature, measured in kPa.

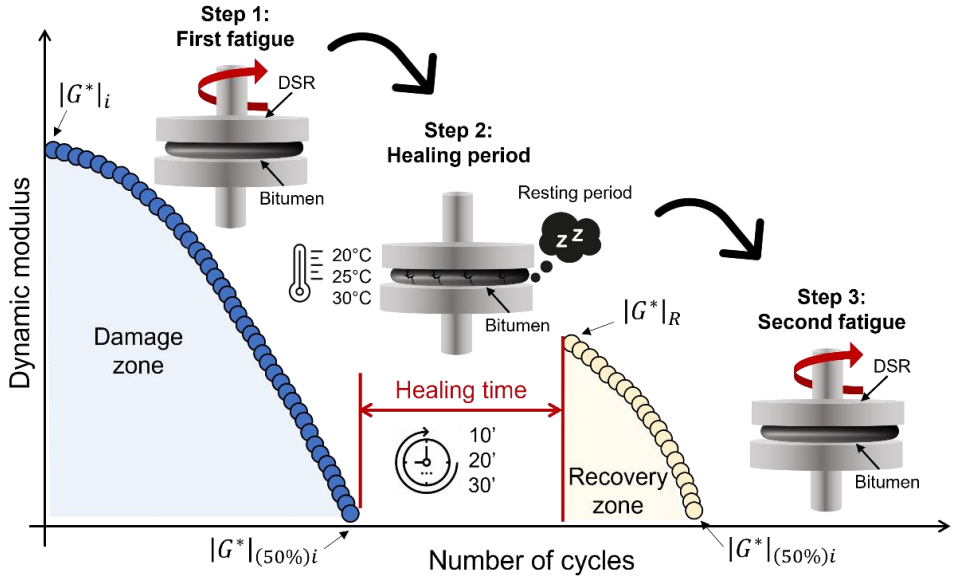

Figure 3. Representation of the self-healing test of bitumen samples in fatigue mode and their theoretical fatigue curves, including the variables $|G^*|_i$, $|G^*|_{(50\%)i}$ and $|G^*|_R$.

2.6. Self-healing level of the rejuvenated bitumen using a strength tensile test

The effect of the type of rejuvenator (PR and CR), rejuvenator dosage (3 and 6 wt.%), healing time (3, 6 and 12h), and healing temperature (15, 20 and 25°C) were also evaluated as independent variables to quantify their effect in the self-healing capacity of aged PAV-aged bitumen. To do that, a mechanical tensile fracture test was designed as follows. For the preparation of the bitumen samples, a mass of 80 g of PAV-aged bitumen was poured into a beaker and then heated to a temperature of 140°C using a hotplate.

Later, the PAV-aged bitumen was mechanically stirred at 300 rpm for 15 minutes. During this process, the PR and CR were incorporated at two different doses: 3% and 6 wt.% total of PAV-aged bitumen. The mixture was then poured into tensile moulds (with the same geometry as the ductility moulds) and allowed to rest until reaching room temperature (~20°C). The healing level in the PAV samples due to the variables described above was measured based on a cyclic process consisting of 3 steps of conditioning-fracture-healing as described below:

***Step 1. Sample conditioning*:** the bitumen PAV test samples were conditioned at a temperature of -5°C for 2 hours, to simulate a brittle fracture due to thermal damage in asphalt pavements (Figure 4(a)).

***Step 2. Fracture generation*:** after step 1, the test samples were fractured into two brittle pieces at a temperature of 5°C under uniaxial tensile testing using a Zwick/Roell Z05 universal testing machine equipped with a 1 kN load cell with a testing thermal chamber and configured at a loading speed of 5 mm/min (Figure 4(b)).

***Step 3. Healing process*:** The fractured pieces were carefully placed back into the mould and secured with bolts at both ends, ensuring that no pressure was applied to the fracture zone (Figure 4(c)). The samples were then conditioned in a thermal chamber at three different healing temperatures, with assessments conducted after 3, 6, and 12 hours of healing time. After the designated healing period, steps 1 and 2 were repeated to determine a healing index through a tensile test (HI_t) according with the following equation:

$$HI_t(\%) = \left(\frac{F_h}{F_i}\right) \times 100 \quad (4)$$

where F_i and F_h are the maximum forces resisted by a sample before and after the healing process, respectively.

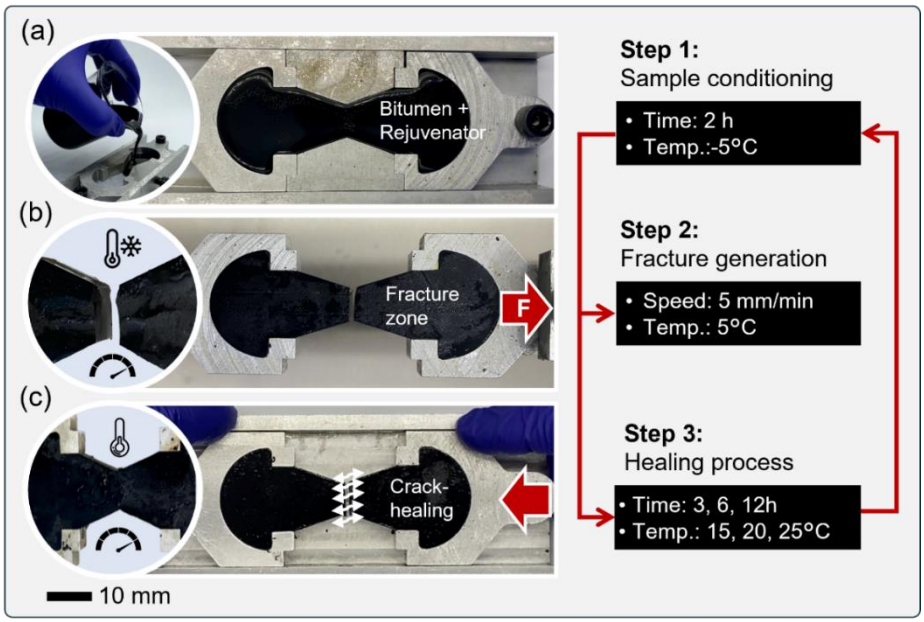

Figure 4. Representation of the cracking self-healing methodology of PAV-aged bitumen and PAV-rejuvenated bitumen containing commercial and pyro-rejuvenators.

2.7. Statistical analysis of the self-healing capacity of the rejuvenator

The combined effects of rejuvenator type, dosage, temperature, and healing time on the self-healing capability of bitumen were statistically evaluated. To this end, we implemented a 3 × 3 × 5 factorial design, as illustrated in Figure 5, to assess the statistically significant effects of individual and combined factors ($\alpha = 0.05$). In addition, Tukey HSD Post-Hoc test was conducted to evaluate pairwise mean comparisons with a significance of $\alpha = 0.05$. All the statistical analyses were performed using the software OriginPro 2024, version 9.95-2024b (OriginLab Corporation, Northampton, MA, USA).

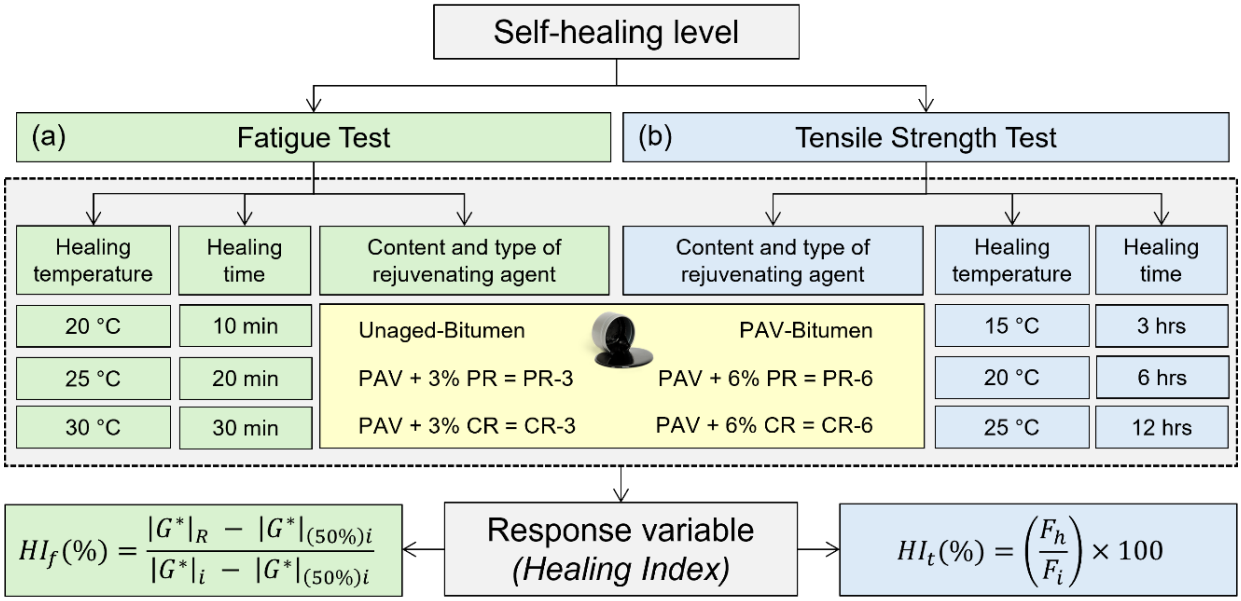

Figure 5: General factorial design variables. (a) Healing Index by fatigue-healing-fatigue test; (b) Healing index by tensile strength test.

3. RESULTS AND DISCUSSION

3.1. Chemical properties of the bitumen blends with and without pyro-rejuvenator

Figure 6a reports GC/MS compositional analysis of the PR and the grouping of components by their major functional groups, namely aromatics, alkenes and others (alkanes, C_{+30} hydrocarbons and poly-aromatics). The results confirm that the PR derived from waste tyres contains a significant proportion of chemical species, such as aromatics and alkenes (combined 94.8% selectivity), which possess potential healing properties. The chemical composition of the pyro-rejuvenator and the commercial rejuvenator (used as a control for self-healing tests), measured by Gas Chromatography coupled with Mass Spectrometry (GC/MS) and FTIR, is presented in Table S1 and Figure S1.

Limonene is a well-known solvent that has demonstrated the ability to restore bitumen properties by inducing the softening of aged bitumen and diffusion to damaged areas [25,39]. Furthermore, this terpene's antioxidant capacity may contribute to the long-term stability of asphalt mixtures used in roads. On the other hand, cymene will add aromaticity to the cracked bitumen, which will help its chemical repair by lowering the ratios of asphaltene to aromatics and resin to aromatics. Both compounds, limonene and cymene, have demonstrated a good diffusion

capacity into asphaltic mixtures and a partial chemical interaction with functional groups in the bitumen´s chemical structure [39]. Thus, the pyro-rejuvenator shows significant potential for self-healing applications in aged bitumen.

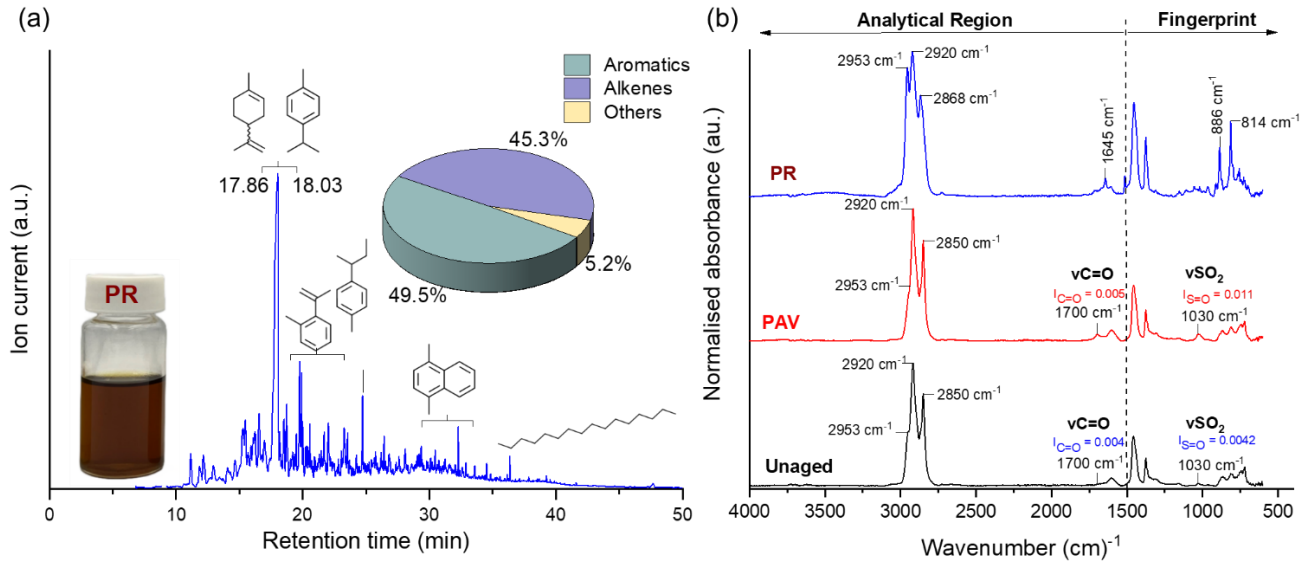

Figure 6. (a) Distribution of products of interest of the pyro-rejuvenator determined by GC/MS; (b) Results of the FTIR-ATR for the unaged bitumen, PAV, and pyro-rejuvenator.

Results from FTIR-ATR (Figure 6b) characterisation of PR were consistent with GC/MS measurements. The intense absorption band at 886 cm^{-1} (Fingerprint region) confirms the presence of limonene, which is also evidenced by the C=C stretching vibrations found at 1645 cm^{-1}.

Moreover, the signal at 814 cm^{-1} is ascribed to C–H out-of-the-plane bending vibrations in aromatics, which is also representative of the cymene molecule. Finally, the strong signals between 2800 cm^{-1} and 3000 cm^{-1} are ascribed to C-H stretching in different hydrocarbon structures with sp^2 and sp^3 hybridisation (alkenes and alkanes).

In the case of the bitumen, the FTIR-ATR spectrums display five absorption bands at 1375, 1455, 2850, 2920, and 2953 cm^{-1}, regardless of their degree of ageing. These bands can be ascribed to C-H vibrations in hydrocarbons, and to alkyl functional groups found in aromatics. Furthermore, there were less prominent signals detected at 1600 cm^{-1} and within the range of 870 to 740 cm^{-1}, which can be attributed to aromatic vibrations. In addition, the absorption bands seen at 1030 cm^{-1} and that at 1700 cm^{-1} for PAV-aged bitumen, corresponds to the bending of the sulfoxide and carbonyl bonds, which are typical descriptors of the ageing in bitumens, which could explain the weakness of these signals in unaged samples.

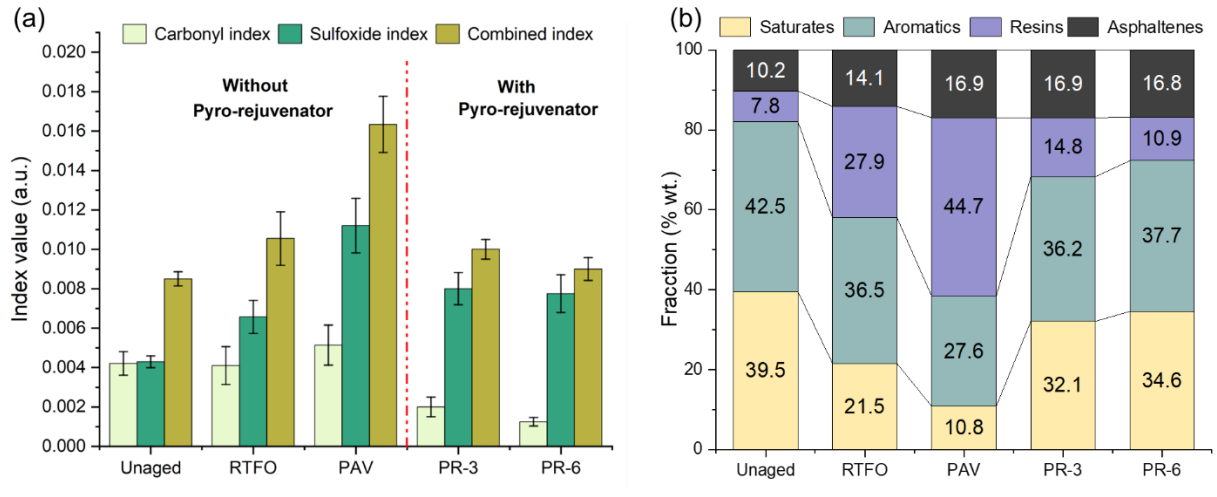

Figure 7: (a) Average results of carbonyl, sulfoxide, and combined ageing indices; (b) SARA fractions for the unaged, RTFO, PAV, PR-3 and PR-6 to bitumen samples.

When mixed with aged bitumen at 3 wt.% or 6 wt.%, the pyro-rejuvenator reduces the combined healing index ($I_{C=O} + I_{SO}$) to a range between the RTFO and unaged samples (Figure 7a). This type of restoration is more pronounced for oxidations involving carbonyls than for those involving sulphur species (see individual indexes). This difference may be attributed to the higher reactivity of sulphur-containing species and the presence of certain sulphur radicals in the pyro-rejuvenator. The chemical effectivity of the pyro-rejuvenator was also confirmed by its effect on SARA composition, where we observed a sharp reduction of asphaltene-to-aromatics and resin-to-aromatic ratios (Figure 7b). This suggests that the pyro-rejuvenator effectively exhibits softening and rejuvenating capabilities, mediated through chemical interactions with the bitumen.

Despite the dosage of the PR was doubled, the results of SARA fractions were not proportional to that increment. This result is in line with previous papers reporting the effect of rejuvenator doses on SARA fraction and it could be associated to the analytical characteristics of SARA methodology, which implies several fractionation steps [36,56].

On the other hand, the presence of solvent species and the low viscosity of the PR indicate that an excess of this liquid could lead to a reduction in the mechanical performance of the healed bitumen. Therefore, in the upcoming sections, we will explore the self-healing effects of pyro-rejuvenators on restoring the mechanical properties of aged bitumen.

3.2. Self-healing capability of pyro-rejuvenator in damaged PAV-bitumen by fatigue testing

Figure 8 shows the average values of the healing index (HI_f) values obtained from fatigue-healing-fatigue tests performed on unaged bitumen and PAV rejuvenated with 3 wt.% and 6 wt.% pyro-rejuvenators, as well as a commercial rejuvenator. These results were evaluated at various healing times (10, 20, and 30 minutes) and temperatures (20, 25, and 30°C).

From Figure 8, it can be observed that unaged bitumen exhibits no significant variations in the healing index (HI_f) at a healing time of 10 minutes, maintaining a recovery rate of 5% regardless of the healing temperature. Moreover, the HI_f, of the unaged bitumen, as measured at temperatures of 20 and 25 ºC, is lower than that recorded for PAV containing PR and CR, irrespective of the dosage or the duration of the healing process. On the opposite, for 30°C healing temperature and 20 and 30 minutes of healing time, the HI_f of the unaged bitumen is similar to that of PAVs containing rejuvenators. The previous results could be explained by the viscoelastic nature of bitumen, which under an increase in temperature would favour the molecular mobility in the SARA fractions, thus increasing the ability to restore the microcracks produced in the bitumen sample during the fatigue phase and consequently improving its self-healing capability [55].

In the same line, an increase in temperature would contribute to a reduction in the mass transfer limitations for PR diffusion and to a higher probability of molecular collisions between the rejuvenator components and the bitumen structure, thus leading to a more effective rejuvenation process. In this context, Quezada et al. [39] recently published an extensive work in which they used FTIR measurements with molecular dynamics simulations as a novel approach to understand the diffusion mechanisms of pyro-oils in asphalt binders with self-healing purposes. The authors identified temperature, contact time, binder viscosity, and rejuvenator composition as critical factors influencing the diffusion process. They further demonstrated that the chemical compounds limonene and cymene play essential roles in this mechanism. Limonene aids in softening the aged bitumen, facilitating the rejuvenator's diffusion into the asphalt, while cymene increases the binder's aromatic index, further enhancing softening through its solvent properties.

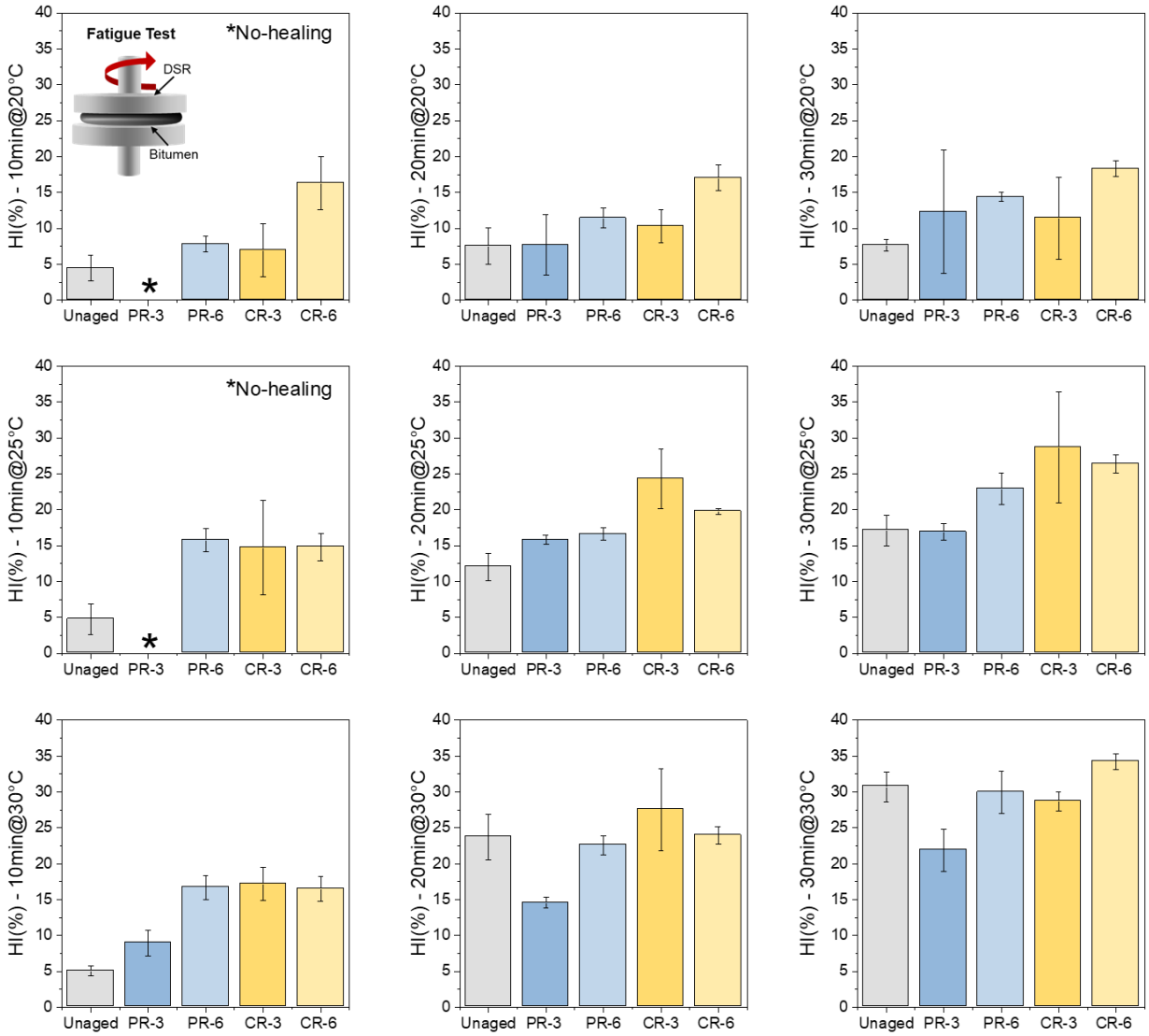

Figure 8: Healing Index (HI_f) by fatigue DSR test for the Unaged, PR-3, PR-6, CR-3, and CR-6 bitumen samples performed at different healing times and temperatures.

On the other hand, when analysing the effect of the dosage and type of rejuvenator (PR or CR) it is observed a similar HI_f between the PR-3 and the unaged bitumen at all combinations of healing times and temperatures. However, with a healing time of 10 minutes at temperatures of 20 and 25°C, PR-3 does not exhibit a rejuvenating effect, indicating no-healing occurs. This suggests that effective material rejuvenation relies on a synergistic interaction among dosage, temperature, and application time to promote successful healing. In contrast, the CR-3 shows a higher HI_f than unaged bitumen at most time-temperature combinations, although with higher variability in HI_f results (SD ~7%).

In the PR-6 sample, the HI_f demonstrated a consistent increase with both healing time and temperature. At 30 °C, healing resulted in 23% and 30% after 20 and 30 minutes, respectively. Under identical conditions, the unaged bitumen exhibited HI_f values of 24% and 31%, suggesting that the aged bitumen treated with PR-6 regained approximately 97% of the healing capacity of the original material, thereby underscoring the rejuvenating effect of PR on PAV-aged bitumen. This remarkable healing capability of the PR at this healing conditions can be attributed to the presence of aromatic species and hydrocarbons, which facilitate the recovery of the saturated and aromatic fractions of aged bitumen (see section 3.1). These chemical families are known for their capability to also promote the softening and diffusion of the pyrolytic rejuvenator into the aged bituminous material, thus improving its mechanical performance [14,25,39]. Furthermore, a comparison of PR-6 with CR-6 shows that both exhibit similar HI_f values across the studied combinations of healing times and temperatures. This confirms that, at this dosage and under the healing conditions evaluated, the pyro-rejuvenator produces effects on aged bitumen comparable to those of its commercial counterpart.

Given the observed impact of the rejuvenating agent on the recovery of the self-healing capability of PAV-aged bitumen, it is crucial to establish a rejuvenation criterion that prevents excessive softening of the material, as this could heighten the susceptibility of the bituminous material to permanent deformation. A reasonable rejuvenation criterion could be defined as the point at which aged bitumen (PAV) demonstrates properties similar to those of virgin bitumen (unaged). The results indicate that the inclusion of PR at a concentration of 6% fulfils this condition, showing a significant rejuvenating effect on aged bitumen, particularly at temperatures of 25 and 30°C, and with an extended healing time (i.e. 30 min).

Table 3 shows the ANOVA *p-values* for each of the studied variables. Overall, the individual factors: type of rejuvenator, rejuvenator doses, and temperature had a statistically significant effect on the HI_f results. In terms of the rejuvenator type, ANOVA results showed that the CR presented a better healing performance than the PR. Regarding the rejuvenator dosage, all the dosages presented a statistically significant effect on the HI_f, where a content 6 wt.% maximised the HI_f. Furthermore, all examined healing temperatures were statistically significant,

with higher temperatures increasing HI_f values. Using CR at a dose of 6 wt.% and a healing temperature of 30°C leads to greater HI_f values across all tested healing timeframes.

Table 3. *P-values* for each of the studied factors and their interactions for the HI evaluated under fatigue test.

Variables	HI@10 min	HI@20 min	HI@30 min
X	<0.0001	<0.0001	0.00515
Y	<0.0001	0.00046	0.00056
Z	0.00023	<0.0001	<0.0001
*X*Y*	<0.0001	0.00070	0.16151
*X*Z*	0.43055	0.53248	0.32302
*Y*Z*	0.02098	0.00025	0.02063
*X*Y*Z*	0.03089	0.04939	0.33194

Notes:

- *X*: Type of rejuvenator (PR, CR); *Y*: Rejuvenator content (0%, 3%, 6%); *Z*: temperature (20°C, 25°C, 30°C).
- *p*-values < 0.05 indicate statistically significant differences.
- Detailed ANOVA results for each healing time can be found in Tables S2 – S4 of the supplementary material.

The simultaneous interaction between factors is also showed in Table 3. Particularly, the double interaction of the rejuvenator type and dosage revealed statistically significant differences on the HI_f at healing times of 10 and 20 min, showing that the CR had a better performance in increasing the HI_f values. However, with a healing time of 30 minutes, no statistically significant difference was observed, meaning that the PR presented HI_f values as high as the CR, regardless of the rejuvenator dosage. For example, with a healing time of 30 minutes at a temperature of 30°C, PR-6 and CR-6 showed average HI_f values of 30.0 and 34.2%, respectively (Figure 8).

Additionally, no statistically significant differences are observed under the simultaneous action of the type of rejuvenator and the healing temperatures evaluated. This finding implies that the PR attained HI_f levels equivalent to the CR during the investigated healing times and temperatures. For example, the average HI_f values for the CR and PR at 30°C were 31.5% and 27.4%, respectively. Additionally, the double interaction between the rejuvenator content and the healing temperature revealed statistically significant differences for each healing time, indicating that, overall, high HI_f were reached at high rejuvenator dosages and temperatures, as expected, regardless of the type of rejuvenator.

Lastly, triple interactions in Table 3 showed statistically significant differences at low and intermediate healing times of 10 and 20 min, while at a high healing time of 30 min, triple interactions were not significant. Thus, at low and intermediate healing times the healing process can be explained by the simultaneous action of the rejuvenator, their dosage and healing temperature. While at high healing times, the simultaneous action of these variables is not significant. So, for instance, the HI_f value for the PR-6 at 30ºC (30.0%) can be comparable with that of the CR-3 at 25ºC (28.7%), CR-3 at 30ºC (28.7%), CR-6 at 25º (26.4%), or even CR-6 at 30º (34.2%). Based on the previous results and statistical analysis, it can be concluded that the healing process of the material is conditioned by the healing time. Furthermore, the best conditions for the use of PR can be its application at a dose of 6 wt.%, and healing temperatures of 30ºC, with HI_f values comparable to the standard CR.

3.3. Self-healing capability of the pyro-rejuvenator in damaged PAV-bitumen by tensile testing

Figure 9 show the average results of the healing indices obtained under tensile test (HI_t) for the bitumen samples depending on the rejuvenator type (PR and CR), rejuvenator content (3 and 6 wt.%), healing time (3, 6 and 12h), and healing temperature (15, 20 and 25ºC). As a reference, Figure 9 shows the PAV-aged sample without rejuvenator for each healing combination. In term of variables of healing time and temperature, from Figure 9 shows that the lowest HI_t values were reached at 3h and 15°C, where the PAV, PR-3, PR-6, CR-3, and CR-6 samples resulted in average HI_t values of 5.2%, 10.2%, 14.7%, 7.1%, and 13.0%, respectively.

The PAV-aged bitumen sample demonstrated a general increase in healing capacity with longer healing times and higher temperatures. For a healing time of 12 hours at a temperature of 25°C, the average HI_t values for the PAV, PR-3, PR-6, CR-3, and CR-6 samples were 25.1%, 98.1%, 102.3%, 88.1%, and 97.1%, respectively. The highest HI_t for the PR-6 over 100% meant that the tensile strength of the bitumen sample after the healing was greater than before the healing process. A reason for this phenomenon can be explained by a greater cohesive effect during the diffusion of the PR through the cracked zone at a high time (12 h) and temperature (25°C). Such conditions promoted the total crack closure of the bitumen sample during the healing process.

Figure 9 also demonstrates that the healing temperature resulted in variations in the HI_t that exceeded those produced by the healing time. Moreover, Figure 9 shows a comparable effect on the rejuvenator type (PR or CR)

418 when analysing the HI_t values at equivalent rejuvenator dosages, independent of the healing time and temperature
419 conditions. The addition of PR exhibited a softening effect similar to that of the standard CR additive, facilitating
420 the diffusion of bitumen and aiding in the closure of microcracks. The results indicate that the PR positively
421 influenced the restoration of the mechanical performance of the bitumen under the evaluated conditions, thereby
422 maximising the HI_t.

423 To quantify the effectiveness of the type of rejuvenator, its dosage, and the healing conditions on the HI_t compared
424 to a reference the PAV-aged sample without rejuvenator, a Healing Index Improvement (HI_i) was determined,
425 according to the equation 5:

$$HI_i(\%) = HI_R - HI_{PAV} \quad (5)$$

426 where the HI_{PAV} and HI_R are the healing indices for the PAV and PAV with rejuvenator addition, respectively.
427 The HI_i results are showed in Figure 10.

428 Figure 10 shows positive HI_i values indicating a healing performance better than PAV-aged bitumen. It can be
429 clearly seen that the HI_i was improved as the healing time and temperature were increased, as expected. A
430 comparison at the same rejuvenator dosage and healing temperature reveals that at low and intermediate healing
431 times of 3 and 6h the differences for the HI_i are higher when compared the PR with the CR. As example, at 6h
432 and 15°C the HI_i values for the CR-3, PR-3 were +1.3% and +9.3%, while the HI_i for the CR6, and PR-6 were
433 +8.7% and +18.3%. In contrast, at a high healing time of 12 h and for 20ºC and temperatures of 20°C and 25°C,
434 the HI_i values for the PR and CR were quite similar. As an example, the HI_i values at 12 h and 25°C for the CR-
435 3, PR-3 were +63.0% and +73.0%, while the HI_i for the CR6, and PR-6 were +72.0% and +77.2%.

436 These results suggest that the healing phenomenon observed under these conditions is driven by a combined effect
437 of rejuvenator dosage, healing time, and healing temperature, with no observable difference between CR and PR.
438 However, a comparison of specific results indicates that PR demonstrates superior overall healing performance
439 compared to CR. Additionally, it can be hypothesised a purer effect of the rejuvenator on the HI_t at low healing
440 times and temperatures. While at high healing times and temperature, the variations in the HI_t are explained by a
441 combination of factors (dosage, time, and temperature). The interactions between the studied factors were

discussed using the analysis of variance (ANOVA) and post-hoc pairwise mean comparisons technique using Tukey, and Table 4 present the *p-values* from the ANOVA for the HI_t parameter considering each of the studied factors and their interactions at the different healing times.

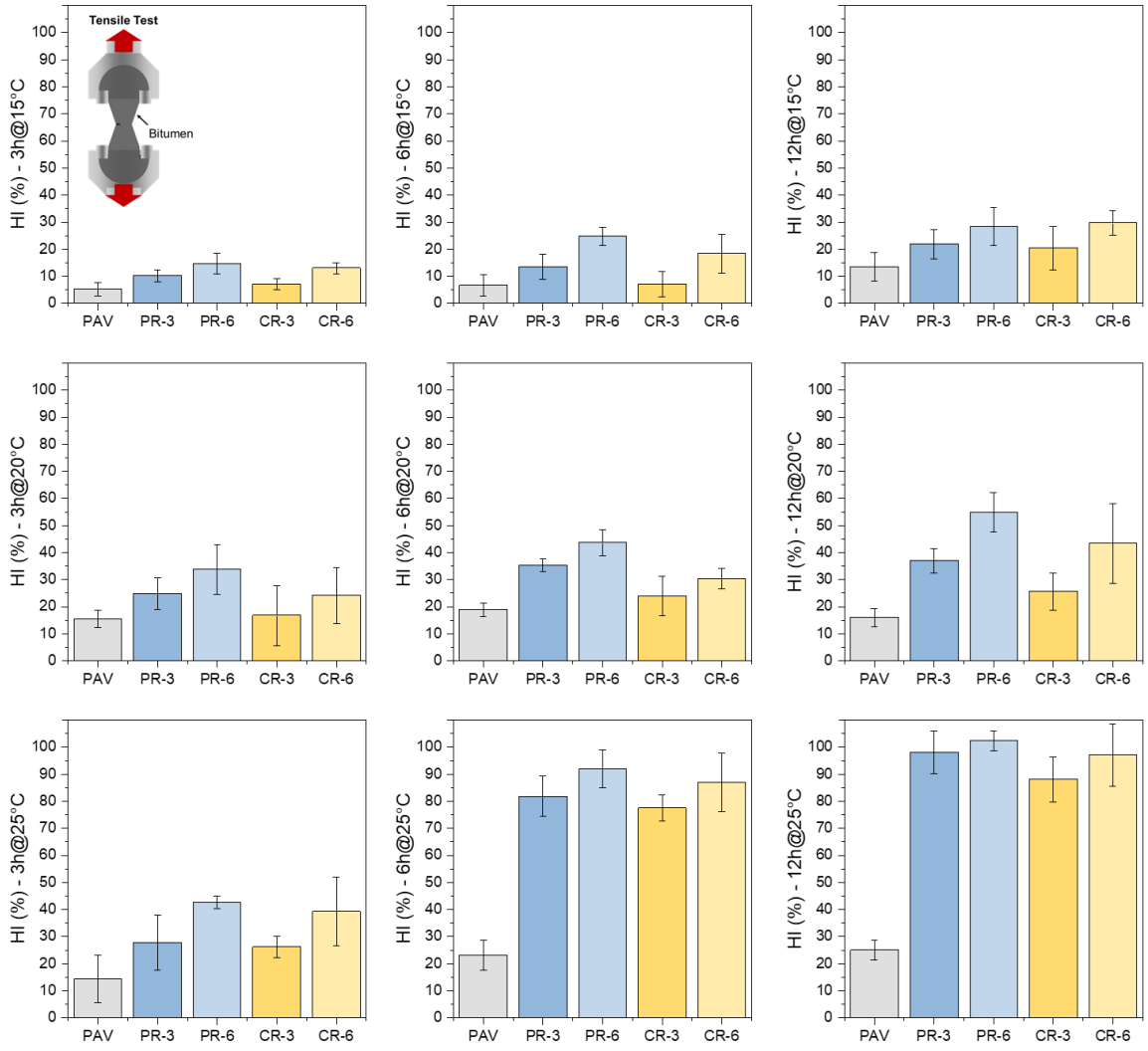

Figure 9. Healing Index (HI_t) obtained from tensile test for the PAV, PR-3, PR-6, CR-3, and CR-6 bitumen samples performed at different healing times and temperatures.

Regarding the effect of the individual factors (see variables *X*, *Y*, and *Z* in Table 4), the results indicates that the rejuvenator type, rejuvenator content, and healing temperature resulted in statistically significant differences for the HI_t, except for the healing time of 3h. At this condition the effect of the type of rejuvenator was not significant in the *HI* (*p-value* 0.11237). Since the type of rejuvenator comprehend two levels (PR or CR), the non-significant

differences previously detected can be explained by the similar HI_t for the PR and CR, with average values of 21.0% and 18.0%, respectively.

Conversely, the variables of rejuvenator content and healing temperature comprehend 3 study levels from which the Tukey pairwise mean comparison revealed that each level resulted in significant differences. These results indicate that each primary factor in the study, along with their respective levels, produced statistically significant changes in the healing performance of the PAV-aged bitumen as evaluated by the tensile test.

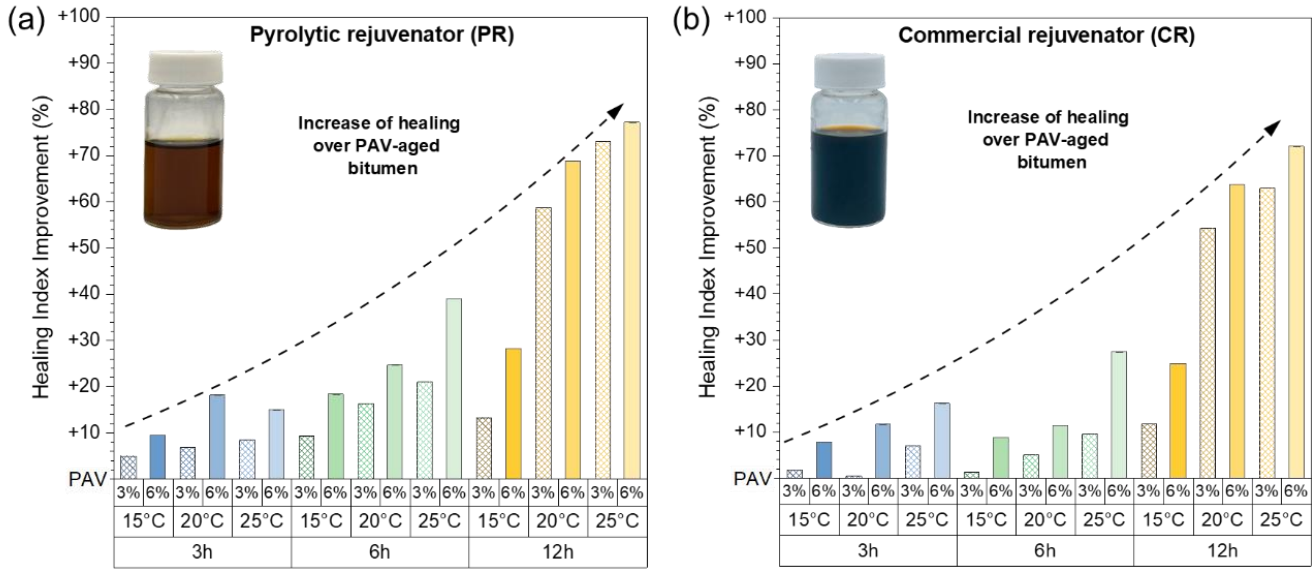

Figure 10: Values of the Healing Index Improvement (HI_i) for the (a) Pyrolytic rejuvenator and (b) Commercial rejuvenator at different healing times, healing temperatures and rejuvenator doses.

In terms of the simultaneous interaction between the studied factors, Table 4 shows that double interactions were not statistically significant, except for the interaction between the rejuvenator content and the healing temperature evaluated at each of the healing times (see Y*Z variable in Table 4).

Additionally, triple interactions were not statistically significant. As previously hypothesised, the Tukey pairwise mean comparison confirmed that the differences in the HI_t between the samples CR-3, PR-3, CR6, and PR-6 were not statistically significant at 25°C for each of the healing times. Thus, the variations identified in the HI_t values are not only explained by the effect of the individual factors itself, but by the combined influence of rejuvenator dosage and healing temperature.

From the previous results, Table 4 reveals a pattern – interactions involving the type of rejuvenator (see X*Y, X*Z, and X*Y*Z) resulted in not statistically significant differences for the HI_t results. Possible implications associated to these results can be that under a realistic scenario, where it is expected that variables interact each other, the use of PR can be as competitive as the CR, representing a sustainable alternative for healing purposes of crack-damaged bituminous materials. This result aligns with previous findings obtained by Chavez Delgado et al. [44], concluding that the PR can restore the rheological properties of aged bitumen samples in a similar way that the CR.

Table 4. *p-values* for each of the studied factors and their interactions for the *HI* evaluated under tensile test.

Variables	***HI*@3h**	***HI*@6h**	***HI*@12h**
X	0.11237	0.00142	0.03211
Y	<0.0001	<0.0001	<0.0001
Z	<0.0001	<0.0001	<0.0001
X*Y	0.51740	0.06135	0.26367
X*Z	0.56782	0.36325	0.26465
Y*Z	0.04349	<0.0001	<0.0001
X*Y*Z	0.95202	0.89421	0.81204

Notes:

- X: Type of rejuvenator (PR, CR); Y: Rejuvenator content (0%, 3%, 6%); Z: temperature (15°C, 20°C, 25°C)
- *p*-values < 0.05 indicate statistically significant differences.
- Detailed ANOVA results for each healing time can be found in Tables S5 – S7 of the supplementary material.

Finally, based on the statistical analysis, it can be concluded that the best experimental conditions to optimise the Healing Index of the bitumen samples, HI_t, are: i) the selection of PR since its similar effect compared to the CR, ii) a rejuvenator dosage of 3 wt. % (average HI_t: 98.12% ± 7.9%) since no difference with a dosage of 6 wt. % (average HI_t: 102.24% ± 3.7%), were observed and iii) a healing temperature and time of 25°C and 12 h, respectively, since at such conditions the HI_t is maximised.

3.4. Morphological analysis AFM images of bitumen with and without pyro-rejuvenator

Figure 11 (a-c) shows the micromorphology of virgin bitumen (unaged), PAV-aged and rejuvenated with 6% PR, obtained through AFM analysis. The images display elongated aggregates, measuring between 2 and 4 μm, with a wavy texture inside and sub-nanometric edges, uniformly distributed throughout the material's matrix. These

aggregates consist of saturated compounds, aromatics, resins and asphaltenes, arranged in a characteristic pattern known as the “bee structure” [57–59].

In unaged bitumen (see Figure 11(a)), the bee structures appear individualised and dispersed, which can be attributed to a higher maltene fraction, facilitating their dispersion across the surface. This behaviour suggests that maltenes play a key role in keeping the bee structures separated, promoting the material's fluidity and, thus, its self-healing capability. In contrast, aged bitumen (see PAV in Figure 11(b)) shows a higher aggregation of bee structures, indicating greater molecular interaction between them. This phenomenon may be associated with the solid fraction of asphaltenes, which possess high polarity and can interact with other compounds in bitumen, resulting in the formation of aggregates [60]. Consequently, the AFM evidence that the reduction of maltenes during ageing limits the dispersion of asphaltenes and induces the formation of clusters between bee structures [59,61].

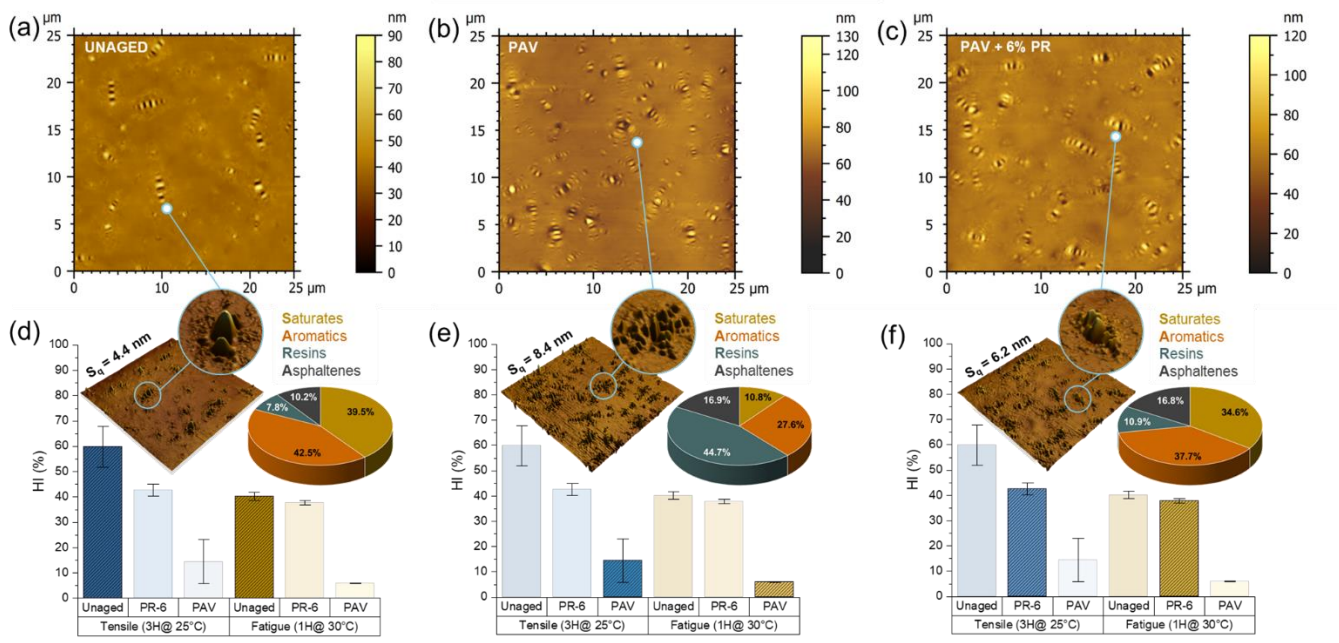

Figure 11. (a-c) 2D AFM images of unaged (virgin bitumen), rejuvenated PAV-aged bitumen with 6% PR and PAV-aged bitumen; and (d-f) 3D AFM images, SARA fractions and Healing Indices (HI) of the bitumen samples.

In the case of bitumen rejuvenated with 6% PR, see Figure 11(c), the bee structures are also observed, although with variable sizes and a more dispersed distribution compared to PAV-aged bitumen. The connections between

these structures appear less intense in the AFM images, suggesting that PR acted as a dispersing agent for the bee-like clusters. This behaviour can be attributed to the restoration of the maltene fraction provided by the PR, which promoted greater separation between asphaltene structures, reducing their molecular interactions [62]. Therefore, it is hypothesised that incorporating 6% PR into the PAV-aged bitumen promotes chemical interactions that operate through several complementary mechanisms. One possible explanation for this phenomenon is that the compounds present in PR, specifically limonene and cymene, may diffuse into the aged bitumen matrix and interact with resins and asphaltenes, leading to a reduction in viscosity and an increase in the material's flexibility. Furthermore, the aromatic compounds in the PR may facilitate the redistribution of asphaltenes, promoting the disruption of their aggregations and enhancing their solubility within the bituminous matrix. Additionally, limonene could act as an antioxidant agent by reacting with oxygenated functional groups formed during ageing, thereby promoting the chemical stabilisation of the bitumen. As a result of these potential mechanisms, the bituminous material undergoes a softening of its asphaltic structure, leading to a reduction in stiffness. This behaviour is reflected in the variation of the physical properties observed in the PAV and PAV + 6% PR bitumen, as shown in Table 2.

In addition, Figure 11(d-f) presents the three-dimensional (3D) AFM reconstructions for each bitumen, characterised by the root mean square average roughness (*Sq*). For a PAV-aged bitumen (see Figure 11(e)), an increase in *Sq* of +90% is observed compared to the virgin bitumen (see Figure 11 (d)). The rise in *Sq* during the ageing process can be attributed to the partial volatilisation of lower molecular weight components associated with the maltene fraction and the increase in higher molecular weight components, such as asphaltenes, forming more rigid and dense structures on the surface. With the incorporation of 6 wt.% PR in the PAV bitumen, a decrease in *Sq* of -26% is evident compared to PAV (see Figure 11(f)), revealing a smoother and more uniform microstructure on the material's surface. This phenomenon is confirmed in the SARA analysis (see Figure 11(d-f)), which shows the oxidation process from the unaged to the PAV-aged state. The asphaltene/maltene ratio increases from 0.114 to 0.203 with PAV ageing, which implies increased stiffness and susceptibility to cracking in the bitumen. With the addition of 6% PR, this ratio is slightly reduced to 0.202, approaching the PAV-aged condition. However, the maltene sub-fractions in PR-6 show remarkable changes; saturates and aromatics increase by 61.0%, while resins

decrease by 75.6% compared to PAV-aged bitumen, achieving a composition similar to unaged bitumen. As the asphaltene fraction remains constant, it is concluded that PR-6 acts as a peptising agent, promoting the dispersion of high polarity asphaltenes in the bitumen matrix, reducing the stiffness of the aged bitumen and relieving internal stresses that produce a softening effect in the bitumen matrix.

From a self-healing perspective and considering that the diffusion process of a rejuvenator primarily depends on molecular mobility, lower roughness in rejuvenated bitumen may enhance molecular mobility. This improvement can, in turn, increase the bitumen's ability to close microcracks autonomously under mechanical stress [63]. The addition of PR facilitates the formation of a less dense and rigid structure, promoting a more flexible matrix that better redistributes internal stresses. This is essential for optimising the pavement's self-healing capacity.

In contrast, aged bitumen, characterised by increased roughness and stiffness, limits molecular mobility and reduces the effectiveness of its self-healing process. This suggests that, although aged bitumen maintains a reduced intrinsic self-healing capacity (quantified in Figure 11 (d-f)), this capacity is significantly increased with the addition of PR. In this context, Quezada et al. [39] demonstrated through molecular dynamics simulations that the limonene and cymene components present in the pyro-oils interact chemically with the asphalt binder, promoting both diffusion and softening of the bituminous matrix. This result indicates that the incorporation of a PR with high percentages of limonene and cymene (see Table S1, supplementary material) could increase the durability of asphalt roads by enhancing the extrinsic self-healing capacity in asphalt roads.

3.5. Effect of adding Pyro-Rejuvenator on the Properties of PAV-Aged Bitumen

To quantify the effect of adding 6% by weight of PR on the physical, chemical, and self-healing properties of PAV-aged bitumen, an Improvement Ratio (IR) was calculated in this section as follows:

$$Improvement\ Ratio\ (\%) = \left(\frac{X_i - X_{Unaged}}{X_{Unaged}}\right) \times 100\ ;\ with\ i = PAV_{aged}\ or\ PAV_{rejuvenated} \quad (6)$$

where X_i and X_{Unaged} are the average results for the Physical (i.e., softening point and AFM rugosity), Chemical (i.e., FTIR combined index, Saturates + Aromatic fractions), and Healing Indices (i.e., obtained via fatigue and tensile tests) obtained to PAV_{aged} or $PAV_{rejuvenated}$, and Unaged Bitumen samples, respectively.

Figure 12 summarises the IR results. As the IR values approach the reference line of the unaged bitumen, whether positive or negative, it indicates that the evaluated property aligns more closely with the behaviour of the virgin bitumen. From Figure 12, it can be seen that the IR values of the PAV-aged sample demonstrate greater magnitudes of physical, chemical, and healing properties compared to the PR-6 sample. These results indicate that incorporating PR into PAV-aged bitumen leads to significant changes in its properties. Specifically, a decrease in softening point and surface roughness suggests improved flexibility and reduced stiffness of the bitumen. Additionally, regarding chemical properties, adding PR lowers oxidation rates and restores the content of saturated and aromatic fractions, which are crucial for binder stability and resistance to oxidative bitumen ageing.

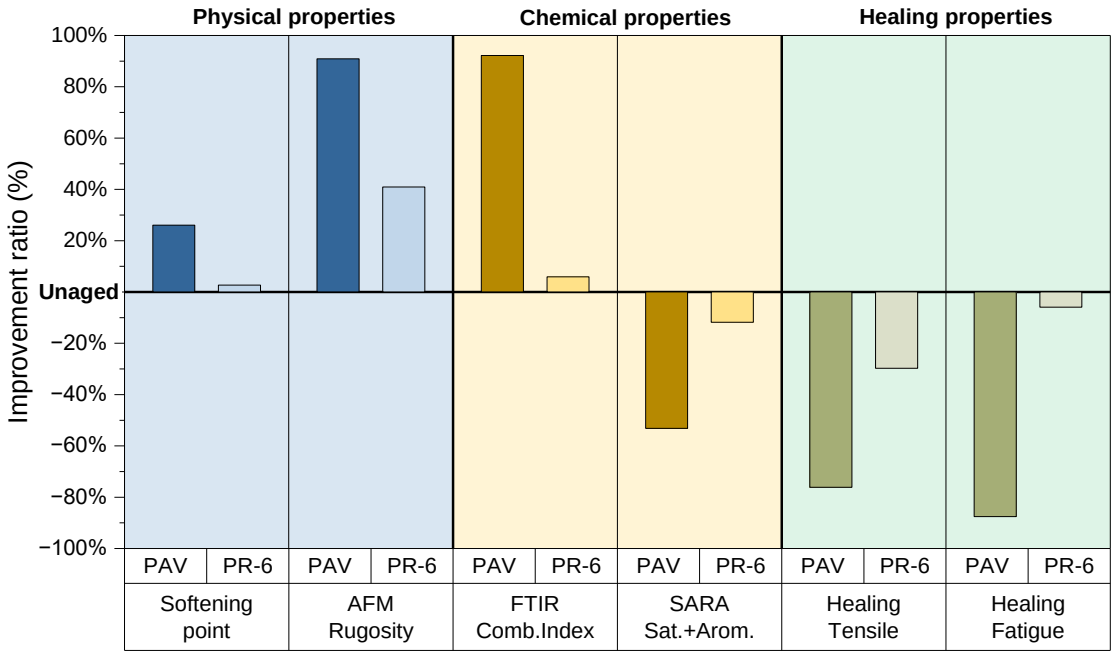

Figure 12. Improvement ratio results for the physical, chemical, and healing properties of the bitumen samples.

Moreover, tensile and fatigue tests show that the incorporation of PR into aged bitumen significantly increases its healing capacity compared to PAV-aged bitumen. This increase in healing parameters, particularly under fatigue conditions, is crucial for the healing process of microcracks, which helps to prevent further damage to asphalt pavements. In conclusion, these combined effects underscore PR's significant potential to enhance both the mechanical and chemical performance of the bitumen. Furthermore, PR contributes to the sustainability of infrastructure construction by decreasing reliance on virgin resources and prolonging the service life of bituminous

materials under the temperature conditions evaluated. This dual benefit positions PR as a crucial innovation in the development of more resilient and environmentally responsible pavement solutions.

4. CONCLUSIONS

This study demonstrates that the pyro-rejuvenator derived from waste tyres significantly enhances the self-healing capacity of aged bitumen. Its composition, rich in aromatics and alkenes—primarily limonene and cymene—facilitates the restoration of maltenic fractions in aged bitumen and reduces carbonyl and sulfoxide groups, both of which are critical to the chemical stability of bitumen used in asphalt binders.

AFM analysis revealed that at a 6 wt.% dosage, the treated bitumen exhibited greater dispersion of "bee-like" structures and reduced surface roughness, indicating a microstructural reconfiguration more closely resembling that of virgin bitumen. This reconfiguration suggests improved molecular mobility, which enhances the material's capacity to activate self-healing mechanisms in response to damage.

Fatigue and tensile tests confirmed that a 6 wt.% dosage of the pyro-rejuvenator enabled a healing index comparable to that of both virgin and commercially rejuvenated bitumen under similar experimental conditions. These healing rates are crucial for the closure of micro-cracks during rest periods, helping to mitigate damage propagation and extend pavement service life.

In summary, the pyro-rejuvenator produced through the pyrolysis and subsequent distillation of waste tyres proves to be a highly effective agent for enhancing the self-healing performance of aged bitumen. These findings support its potential as a sustainable alternative for road infrastructure rehabilitation, contributing simultaneously to waste valorisation in civil engineering applications.

Declaration of Competing Interest

The authors declare that they have no known competing financial interests or personal relationships that could have appeared to influence the work reported in this paper.

CRediT authorship contribution statement

Manuel Chávez-Delgado: Methodology, Investigation & writing-original draft preparation and editing, **Jose L Concha:** Data curation, validation, conceptualisation, and writing-original draft preparation, **Silvia Caro**: data analysis and writing-original draft preparation, **Carlos P. Silva:** Data curation, **Luis E. Arteaga-Pérez:** Conceptualisation, methodology, supervision, and writing-original draft preparation, **Jose Norambuena-Contreras:** Supervision, funds acquisition, conceptualisation, and writing-original draft preparation.

ACKNOWLEDGEMENTS

The authors would like to acknowledge the financial support provided by the National Research and Development Agency (ANID) through the Research Project FONDEF IDeA 21I10127 and FONDEQUIP EQM160036. Additionally, the first author extends thanks to the Universidad del Bío-Bío for the internal PhD scholarship awarded. The second author would like to thank the financial support provided by the Universidad del Bío-Bío through the FAPEI FP2441850. Finally, the authors express their gratitude to María Paula Perilla, a student from the University of the Andes in Colombia, for her technical support throughout the testing program.

REFERENCES

[1] Gonzalez-Torre I, Norambuena-Contreras J. Recent advances on self-healing of bituminous materials by the action of encapsulated rejuvenators. Constr Build Mater 2020;258:119568. https://doi.org/10.1016/j.conbuildmat.2020.119568.

[2] Hu Y, Si W, Kang X, Xue Y, Wang H, Parry T. State of the art: Multiscale evaluation of bitumen ageing behaviour. Fuel 2022;326. https://doi.org/10.1016/j.fuel.2022.125045.

[3] Li F, Wang Y, Miljković M, Chan KM. Changes in the nanoscale asphaltene particles and relaxation spectra of asphalt binders during aging and rejuvenation. Mater Des 2022;219. https://doi.org/10.1016/j.matdes.2022.110808.

[4] Behnood A. Application of rejuvenators to improve the rheological and mechanical properties of asphalt binders and mixtures : A review. J Clean Prod 2019;231:171–82. https://doi.org/10.1016/j.jclepro.2019.05.209.

[5] Concha JL, Delgadillo R, Arteaga-Pérez LE, Segura C, Norambuena-Contreras J. Optimised Sunflower Oil Content for Encapsulation by Vibrating Technology as a Rejuvenating Solution for Asphalt 2023.

[6] Wang J, Wang T, Hou X, Xiao F. Modelling of rheological and chemical properties of asphalt binder considering SARA fraction. Fuel 2019;238:320–30. https://doi.org/10.1016/j.fuel.2018.10.126.

[7] Wang X, Guo G, Zou F, Zhao H, Li Y. Enhancing self-healing properties of microcrack on aged asphalt incorporating with microcapsules encapsulating rejuvenator. Constr Build Mater 2022;344. https://doi.org/10.1016/j.conbuildmat.2022.128123.

[8] Li J, Ji X ping, Fang X zheng, Hu Y lin, Hua W long, Zhang Z ming, et al. Self-healing performance and prediction model of microcapsule asphalt. Constr Build Mater 2022;330. https://doi.org/10.1016/j.conbuildmat.2022.127085.

[9] Tabaković A, Schlangen E. Self-healing technology for asphalt pavements. Advances in Polymer Science, vol. 273, Springer New York LLC; 2016, p. 285–306. https://doi.org/10.1007/12_2015_335.

[10] Yang P, Wang L, Gao X, Wang S, Su J. Smart Self-Healing Capability of Asphalt Material Using Bionic Microvascular Containing Oily Rejuvenator 2021:1–20.

[11] Gulzar S, Fried A, Preciado J, Castorena C, Underwood S, Habbouche J, et al. Towards sustainable roads: A State-of-the-art review on the use of recycling agents in recycled asphalt mixtures. J Clean Prod 2023;406. https://doi.org/10.1016/j.jclepro.2023.136994.

[12] Anupam BR, Sahoo UC, Chandrappa AK. A methodological review on self-healing asphalt pavements. Constr Build Mater 2022;321. https://doi.org/10.1016/j.conbuildmat.2022.126395.

[13] García Á, Schlangen E, van de Ven M, Sierra-Beltrán G. Preparation of capsules containing rejuvenators for their use in asphalt concrete. J Hazard Mater 2010;184:603–11. https://doi.org/10.1016/j.jhazmat.2010.08.078.

[14] Chávez-Delgado M, Colina JR, Segura C, Álvarez C, Osorio-Vargas P, Arteaga-Pérez LE, Norambuena-Contreras J. Asphalt pyro-rejuvenators based on waste tyres: an approach to improve the rheological and self-healing properties of aged binders. J Clean Prod 2024:142179. https://doi.org/10.1016/j.jclepro.2024.142179.

[15] Li R, Chen J, Zhou T, Pei J. Preparation and characterization of novel light induced self-healing materials for cracks in asphalt pavements. Constr Build Mater 2016;105:336–42. https://doi.org/10.1016/j.conbuildmat.2015.12.004.

[16] Rathore M, Haritonovs V, Merijs Meri R, Zaumanis M. Rheological and chemical evaluation of aging in 100% reclaimed asphalt mixtures containing rejuvenators. Constr Build Mater 2022;318:126026. https://doi.org/10.1016/j.conbuildmat.2021.126026.

[17] Hu D, Gu X, Dong Q, Lyu L, Cui B, Pei J. Investigating the bio-rejuvenator effects on aged asphalt through exploring molecular evolution and chemical transformation of asphalt components during oxidative aging and regeneration. J Clean Prod 2021;329. https://doi.org/10.1016/j.jclepro.2021.129711.

[18] Concha JL, Arteaga-Pérez LE, Gonzalez-Torre I, Liu Q, Norambuena-Contreras J. Biopolymeric Capsules Containing Different Oils as Rejuvenating Agents for Asphalt Self-Healing : A Novel Multivariate Approach 2022:1–20.

[19] Williams PT. Pyrolysis of waste tyres : A review. Waste Management 2013;33:1714–28. https://doi.org/10.1016/j.wasman.2013.05.003.

[20] Sharma A, Sawant RJ, Sharma A, Joshi JB, Jain RK, Kasilingam R. Valorisation of End-of-Life tyres for generating valuable resources under circular economy. Fuel 2022;314:123138. https://doi.org/10.1016/j.fuel.2022.123138.

[21] Antoniou N, Zabaniotou A. Features of an efficient and environmentally attractive used tyres pyrolysis with energy and material recovery. Renewable and Sustainable Energy Reviews 2013;20:539–58. https://doi.org/10.1016/j.rser.2012.12.005.

[22] Meng J, Moore A, Tilotta D, Kelley S, Park S. Toward Understanding of Bio-Oil Aging: Accelerated Aging of Bio-Oil Fractions 2018.

[23] Norambuena-Contreras J, Arteaga-Perez LE, Guadarrama-Lezama AY, Briones R, Vivanco JF, Gonzalez-Torre I. Microencapsulated bio-based rejuvenators for the self-healing of bituminous materials. Materials 2020;13. https://doi.org/10.3390/ma13061446.

[24] Menares T, Herrera J, Romero R, Osorio P, Arteaga-Pérez LE. Waste tires pyrolysis kinetics and reaction mechanisms explained by TGA and Py-GC / MS under kinetically-controlled regime 2020;102:21–9. https://doi.org/10.1016/j.wasman.2019.10.027.

[25] Norambuena-Contreras J, Arteaga-Pérez LE, Concha JL, Norambuena-Contreras J. Pyrolytic oil from waste tyres as a promising encapsulated rejuvenator for the extrinsic self- healing of bituminous materials 2021. https://doi.org/10.1080/14680629.2021.1907216.

[26] Martínez JD, Puy N, Murillo R, García T, Navarro MV, Mastral AM. Waste tyre pyrolysis - A review. Renewable and Sustainable Energy Reviews 2013;23:179–213. https://doi.org/10.1016/j.rser.2013.02.038.

[27] Campuzano F, Martínez JD, Agudelo Santamaría AF, Sarathy SM, Roberts WL. Pursuing the End-of-Life Tire Circularity: An Outlook toward the Production of Secondary Raw Materials from Tire Pyrolysis Oil. Energy & Fuels 2023. https://doi.org/10.1021/acs.energyfuels.3c00847.

[28] Qiu X, Cheng W, Xu W, Xiao S, Yang Q. Fatigue evolution characteristic and self-healing behaviour of asphalt binders. International Journal of Pavement Engineering 2022;23:1459–70. https://doi.org/10.1080/10298436.2020.1806277.

[29] Lv H, Liu H, Zhang C, Wang Y, Han M, Tan Y. Characterization of the healing potential of asphalt binders with separation of thixotropy after cyclic loading. Constr Build Mater 2023;370. https://doi.org/10.1016/j.conbuildmat.2023.130686.

[30] Chávez-Delgado M, Concha JL, Arteaga-Pérez LE, Norambuena-Contreras J. Rejuvenator Based on Pyrolysis of Waste Tyres to Improve Aged Asphalt Rheological Properties. RILEM Bookseries, vol. 58, Springer Science and Business Media B.V.; 2024, p. 140–7. https://doi.org/10.1007/978-3-031-72134-2_14.

[31] Yousefi AA, Ait-Kadi A, Roy C. Effect of used-tire-derived pyrolytic oil residue on the properties of polymer-modified asphalts. n.d.

[32] Sun DX, Zou Y, Wang H, Weng HX. Study of road bitumen modified with heavy fraction of tire pyrolysis oil. Energy Sources, Part A: Recovery, Utilization and Environmental Effects 2011;33:1822–31. https://doi.org/10.1080/15567030903419489.

[33] Ržek L, Ravnikar Turk M, Tušar M. Increasing the rate of reclaimed asphalt in asphalt mixture by using alternative rejuvenator produced by tire pyrolysis. Constr Build Mater 2020;232. https://doi.org/10.1016/j.conbuildmat.2019.117177.

[34] Al-Sabaeei A, Napiah M, Sutanto M, Habib NZ, Bala N, Kumalasari I. Application of nano silica particles to improve high-temperature rheological performance of tyre pyrolysis oil-modified bitumen. Road Materials and Pavement Design 2022;23:1999–2017. https://doi.org/10.1080/14680629.2021.1945483.

[35] Herndon RM, Balasubramanian J, Woelk K, Abdelrahman M. Physical and Chemical Methods to Assess Performance of TPO-Modified Asphalt Binder. Applied Sciences (Switzerland) 2024;14. https://doi.org/10.3390/app14083300.

[36] Fini EH, Hosseinnezhad S, Oldham DJ, Brajendra K. Investigating the effectiveness of liquid rubber as a modifier for asphalt binder 2016;0629. https://doi.org/10.1080/14680629.2015.1124800.

[37] Kumar A, Choudhary R, Kumar A. Evaluation of Waste Tire Pyrolytic Oil as a Rejuvenation Agent for Unmodified, Polymer-Modified, and Rubber-Modified Aged Asphalt Binders. Journal of Materials in Civil Engineering 2022;34. https://doi.org/10.1061/(asce)mt.1943-5533.0004400.

[38] Kumar A, Asce SM, Choudhary R, Ph D, Asce AM, Kumar A. Composite Asphalt Modification with Waste EPDM Rubber and Tire Pyrolytic Oil : Rheological , Chemical , and Morphological Evaluation 2022;34:1–17. https://doi.org/10.1061/(ASCE)MT.1943-5533.0004468.

[39] Quezada GR, Solar C, Saavedra JH, Petit K, Martin-Martínez FJ, Arteaga-Pérez LE, Norambuena-Contreras J. Operando FTIR-ATR with molecular dynamic simulations to understand the diffusion mechanism of waste tire-derived pyrolytic oil for asphalt self-healing. Fuel 2024;357. https://doi.org/10.1016/j.fuel.2023.129834.

[40] Al-Sabaeei AM, Napiah MB, Sutanto MH, Alaloul WS, Yusoff NIM, Khairuddin FH. Evaluation of the high-temperature rheological performance of tire pyrolysis oil-modified bio-asphalt. International Journal of Pavement Engineering 2022;23:4007–22. https://doi.org/10.1080/10298436.2021.1931200.

[41] Avsenik L, Klinar D, Tušar M, Perše LS. Use of modified slow tire pyrolysis product as a rejuvenator for aged bitumen. Constr Build Mater 2016;120:605–16. https://doi.org/10.1016/j.conbuildmat.2016.05.140.

[42] Kumar A, Choudhary R, Kumar A. Composite asphalt binder modification with waste Non-tire automotive rubber and pyrolytic oil. Mater Today Proc 2022;61:158–66. https://doi.org/10.1016/j.matpr.2021.07.431.

[43] Al-Sabaeei A, Napiah M, Sutanto M, Habib NZ, Bala N, Kumalasari I, et al. Application of nano silica particles to improve high-temperature rheological performance of tyre pyrolysis oil-modified bitumen. Road Materials and Pavement Design 2022;23:1999–2017. https://doi.org/10.1080/14680629.2021.1945483.

[44] Chávez-Delgado M, Concha JL, Caro S, Arteaga-Pérez LE, Norambuena-Contreras J. Enhancing rheological and self-healing properties of aged bitumen using a pyro-rejuvenator from waste tyres. Constr Build Mater 2025;470. https://doi.org/10.1016/j.conbuildmat.2025.140639.

[45] Liu L, Li C, Deng Q, Gan Y, Liao W. Study on the high-temperature performance and self-healing capability of asphalt modified with pyrolysis oil from waste tires and polyphosphoric acid. Case Studies in Construction Materials 2024;20. https://doi.org/10.1016/j.cscm.2024.e03291.

[46] Arteaga-Pérez LE, Larrere S, Chávez-Delgado M, Rueda Ordoñez YJ, Concha JL, Segura C, et al. Environmental life cycle assessment of encapsulated rejuvenators from mining truck waste tires via pyrolysis for asphalt self-healing. J Clean Prod 2025;490. https://doi.org/10.1016/j.jclepro.2025.144787.

[47] Yasar A, Rana S, Moniruzzaman M, Nazar M, Tabinda AB, Haider R, et al. Quality and environmental impacts of oil production through pyrolysis of waste tyres. Environ Technol Innov 2021;23. https://doi.org/10.1016/j.eti.2021.101565.

[48] Zabaniotou A, Antoniou N, Bruton G. Analysis of good practices, barriers and drivers for ELTs pyrolysis industrial application. Waste Management 2014;34:2335–46. https://doi.org/10.1016/j.wasman.2014.08.002.

[49] D2872 DA. Standard test method for effect of heat and air on a moving film of asphalt (rolling thin-film oven test). American Society for Testing and Materials, West Conshohocken, PA 2012:1–11.

[50] ASTM D6521. Standard Practice for Accelerated Aging of Asphalt Binder Using a Pressurized Aging Vessel (PAV) Standard Practice for Accelerated Aging of Asphalt Binder Using a Pressurized Aging Vessel (PAV) 2022:1–6.

[51] Standard Test Methods for Separation of Asphalt into Four Fractions 1. n.d.

[52] Concha JL, Arteaga-Pérez LE, Alpizar-Reyes E, Segura C, Gonzalez-Torre I, Kanellopoulos A, et al. Effect of rejuvenating oil type on the synthesis and properties of alginate-based polynuclear capsules for asphalt self-healing 2022. https://doi.org/10.1080/14680629.2022.2092026.

[53] Hu Y, Yin Y, Sreeram A, Si W, Airey GD, Li B, et al. Atomic force microscopy (AFM) based microstructural and micromechanical analysis of bitumen during ageing and rejuvenation. Constr Build Mater 2025;467. https://doi.org/10.1016/j.conbuildmat.2025.140387.

[54] Li J, Ji X ping, Fang X zheng, Hu Y lin, Hua W long, Zhang Z ming, et al. Self-healing performance and prediction model of microcapsule asphalt. Constr Build Mater 2022;330. https://doi.org/10.1016/j.conbuildmat.2022.127085.

[55] Wang B, Shen J, Li S, Wang W. Peanut Shell Powder as a Sustainable Modifier and Its Influence on Self-Healing Properties of Asphalt. Materials 2023;16. https://doi.org/10.3390/ma16206618.

[56] Eltwati A, Al-Saffar Z, Mohamed A, Rosli Hainin M, Elnihum A, Enieb M. Synergistic effect of SBS copolymers and aromatic oil on the characteristics of asphalt binders and mixtures containing reclaimed asphalt pavement. Constr Build Mater 2022;327. https://doi.org/10.1016/j.conbuildmat.2022.127026.

[57] Loise V, Calandra P, Abe AA, Porto M, Oliviero Rossi C, Davoli M, et al. Additives on aged bitumens: What probe to distinguish between rejuvenating and fluxing effects? J Mol Liq 2021;339:116742. https://doi.org/10.1016/j.molliq.2021.116742.

[58] Hung AM, Fini EH. AFM study of asphalt binder “bee” structures: origin, mechanical fracture, topological evolution, and experimental artifacts. RSC Adv 2015;5:96972–82. https://doi.org/10.1039/c5ra13982a.

[59] Zhang H, Wang Y, Yu T, Liu Z. Microstructural characteristics of differently aged asphalt samples based on atomic force microscopy (AFM). Constr Build Mater 2020;255. https://doi.org/10.1016/j.conbuildmat.2020.119388.

[60] Yu T, Wang J, Zhang H, Sun J. Statistical analysis of aging micro-characteristics for asphalt binder AFM images based on neural network classification. Fuel 2024;371. https://doi.org/10.1016/j.fuel.2024.132080.

[61] Primerano K, Mirwald J, Hofko B. Asphaltenes and maltenes in crude oil and bitumen: A comprehensive review of properties, separation methods, and insights into structure, reactivity and aging. Fuel 2024;368. https://doi.org/10.1016/j.fuel.2024.131616.

[62] Ahmad M, Khedmati M, Mensching D, Hofko B, F. Haghshenas H. Aging characterization of asphalt binders through multi-aspect analyses: A critical review. Fuel 2024;376. https://doi.org/10.1016/j.fuel.2024.132679.

[63] He Y, Xiong K, Zhang J, Guo F, Li Y, Hu Q. A state-of-the-art review and prospectives on the self-healing repair technology for asphalt materials. Constr Build Mater 2024;421. https://doi.org/10.1016/j.conbuildmat.2024.135660.